Clase 6 b – Microscopías de 2da armónica

Sabemos que los materiales centrosimétricos no tienen SHG ya que $\chi^{(2)}_{bulk} = 0$, pero esa simetría se pierde en:

Superficies, interfases

Capas moleculares orientadas en superficies

hiperpolarizabilidad

Microscopía con detección de bordes
Muy apreciada en biología, porque se puede usar una longitud de onda que no se absorbe. Bajo daño.
Hay material biológico con mucha señal de SHG cuando forma fibras ordenadas, como el colágeno

$$\eta = \frac{I(2\omega)}{I(\omega)}$$

Δt	Pulse Period
E	Energy per Pulse
f_{rep}	Repetition Rate
P_{avg}	Average Power
P_{peak}	Peak Power
τ	Pulse Width

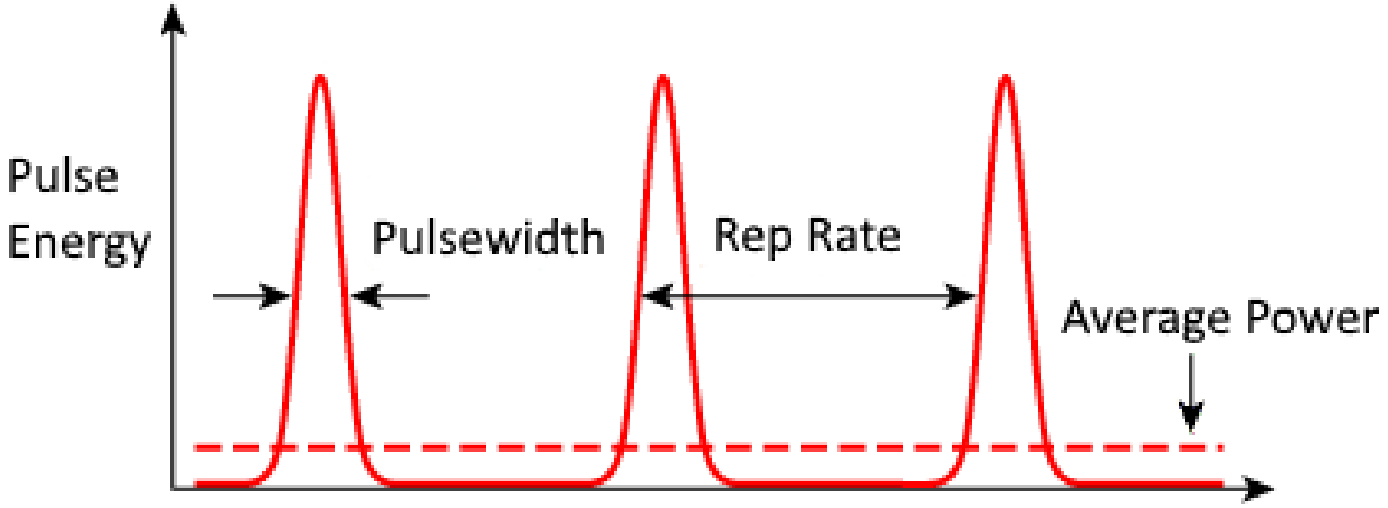

$$P_{peak} = \frac{P_{avg}}{f_{rep} \cdot \tau} = \frac{P_{avg} \cdot \Delta t}{\tau}$$

Second harmonic generation microscopy for quantitative analysis of collagen fibrillar structure

Xiyi Chen[1], Oleg Nadiarynkh[1,2], Sergey Plotnikov[1,2] & Paul J Campagnola[1]

[1]Department of Biomedica l Engineering, University of Wisconsin-Madison, Madison, Wisconsin, USA. [2]Present addresses: Department of Physics, University of Utrecht, Utrecht, The Netherlands (O.N.); US National Institutes of Health, Heart, Lung and Blood Institute, Bethesda, Maryland, USA (S.P.). Correspondence should be addressed to P.J.C. (pcampagnola@wisc.edu).

Published online 8 March 2012; doi:10.1038/nprot.2012.009

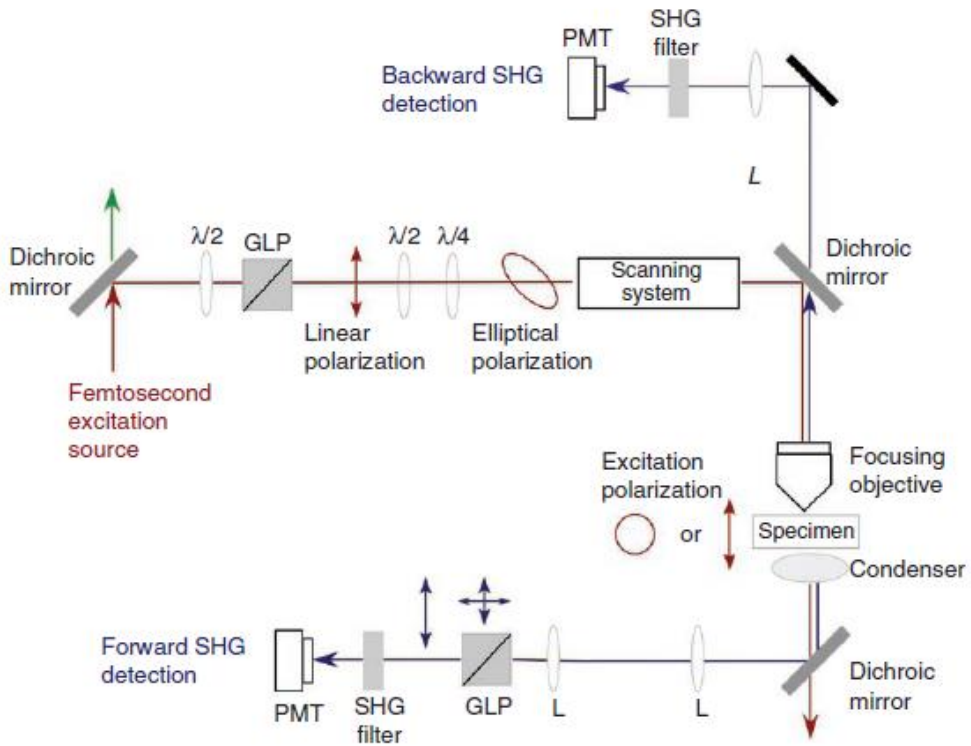

Figure 2 | Schematic of the optical layout of the SHG microscope, showing the optical components before the scan head and the detection pathways. L, lens; λ/2 and λ/4 are half- and quarter-wave plates, respectively.

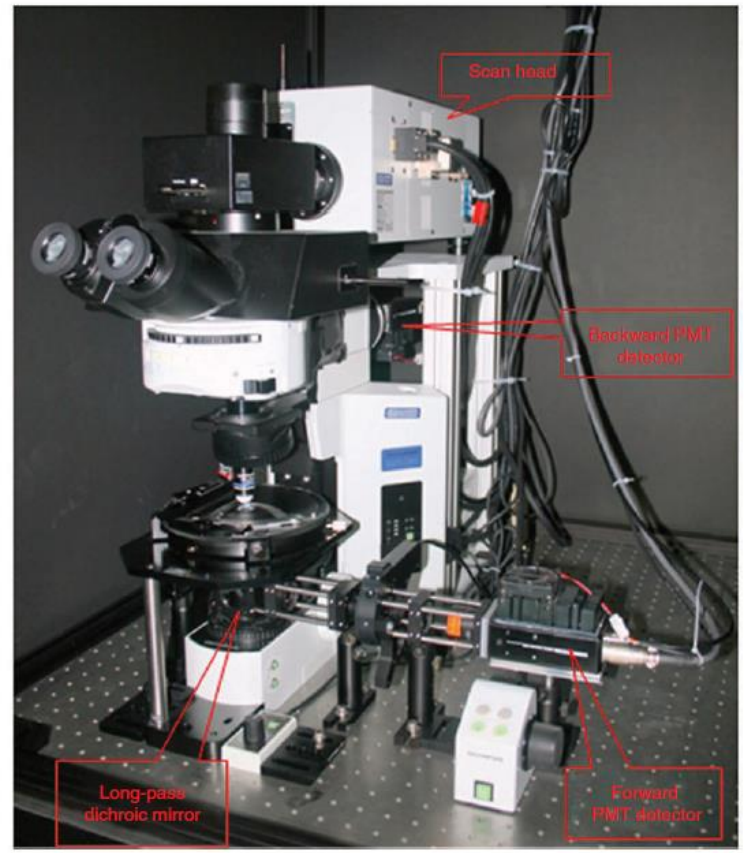

Figure 4 | Annotated photograph of the upright microscope, detectors and light-tight box.

Second harmonic generation microscopy for quantitative analysis of collagen fibrillar str

Xiyi Chen[1], Oleg Nadiarynkh[1,2], Sergey Plotnikov[1,2] & Paul J Campagnola[1]

[1]Department of Biomedica l Engineering, University of Wisconsin-Madison, Madison, Wisconsin, USA. [2]Present addresses: Department of Phy Utrecht, The Netherlands (O.N.); US National Institutes of Health, Heart, Lung and Blood Institute, Bethesda, Maryland, USA (S.P.). Correspo to P.J.C. (pcampagnola@wisc.edu).

Published online 8 March 2012; doi:10.1038/nprot.2012.009

$$\chi^{(2)} = N_s < \beta >$$

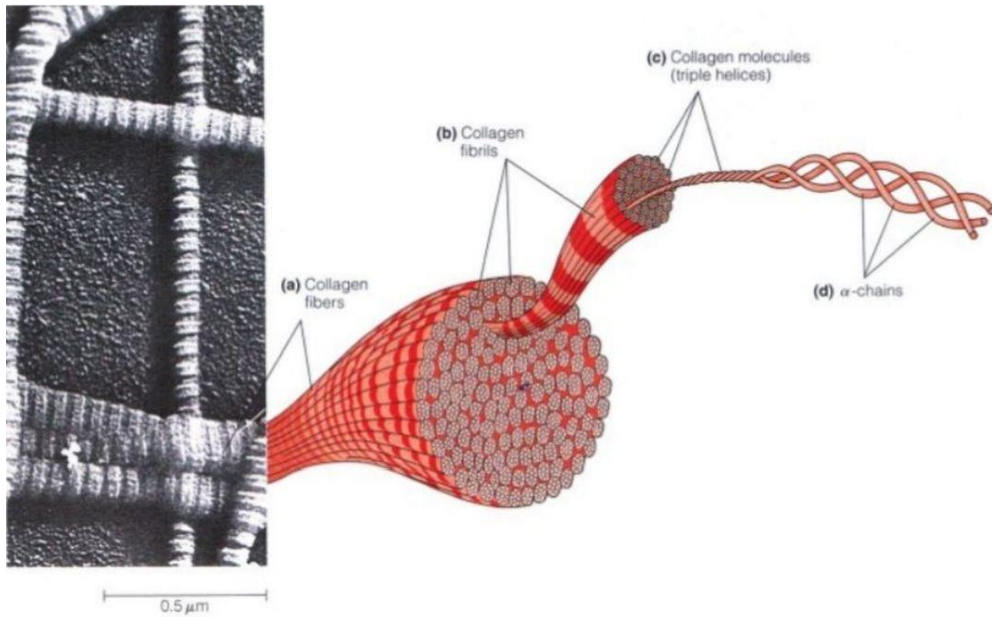

TABLE 1 | Representative example applications of SHG.

Application	Subspecialty	Representative refs.	Key conclusions/observations
Cancer	Breast	6	SHG can delineate cancers of different stages
		7	
		8	
	Ovary	9	SHG shows an increase in collagen fibril/fiber organization
		10	
	Skin	21	SHG can delineate tumor boundaries in different types of skin cancer
		22	
		23	
		24	
Fibrosis	Liver	14	SHG results agree with standard pathology
	Kidney	13	SHG results agree with standard pathology
Connective tissues and disorders	Osteogenesis imperfecta	11	SHG delineates normal and diseased states in several tissue types
	Sjogren's syndrome	12	SHG shows disorganized collagen in this disease
	Cornea	18	SHG can delineate the stroma from other corneal components
		20	
	Skin damage	17	SHG uniquely shows changes in collagen assembly upon thermal damage
Atherosclerosis		15	SHG shows that collagen plaques intermingle with elastin
		16	
Model tissues		19	Self-assembled fibrillar gels can be imaged by SHG
		25	
Theory		26	Theoretical treatments have been developed to understand the SHG emission properties in tissues
		27	
		28	

Second harmonic generation microscopy for quantitative analysis of collagen fibrillar str

Xiyi Chen[1], Oleg Nadiarynkh[1,2], Sergey Plotnikov[1,2] & Paul J Campagnola[1]

[1]Department of Biomedica l Engineering, University of Wisconsin-Madison, Madison, Wisconsin, USA. [2]Present addresses: Department of Phy Utrecht, The Netherlands (O.N.); US National Institutes of Health, Heart, Lung and Blood Institute, Bethesda, Maryland, USA (S.P.). Correspo to P.J.C. (pcampagnola@wisc.edu).

Published online 8 March 2012; doi:10.1038/nprot.2012.009

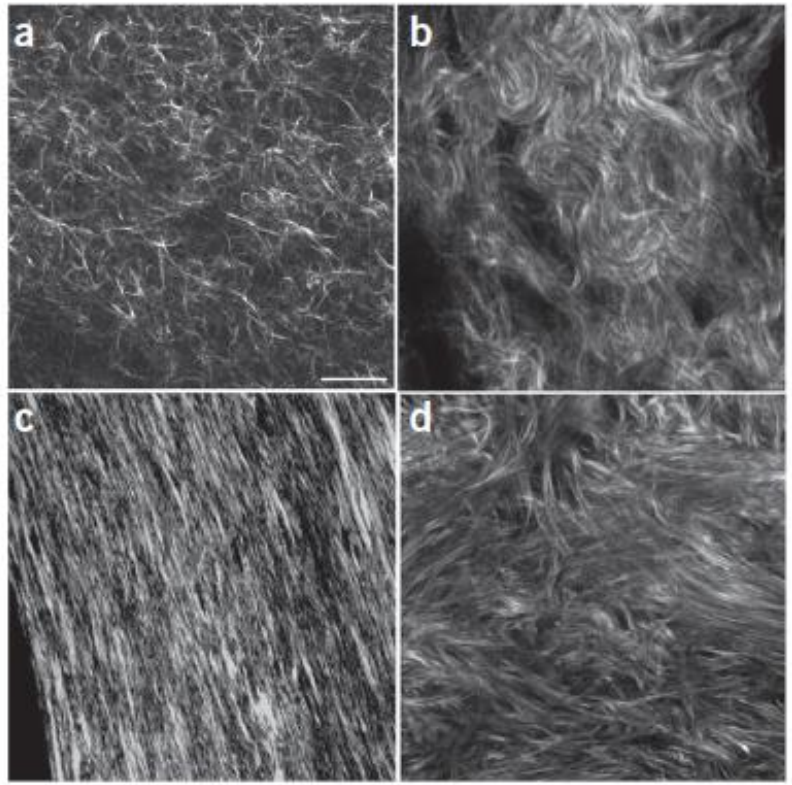

Figure 1 | Montage of SHG imaging of collagen tissues. (**a**–**d**) The single optical sections show representative images of self-assembled collagen gel (**a**); mouse dermis (**b**); mouse bone (**c**); and human ovary (**d**). Scale bar, 30 μm.

TABLE 1 | Representative example applications of SHG.

Application	Subspecialty	Representative refs.	Key conclusions/observations
Cancer	Breast	6	SHG can delineate cancers of different stages
		7	
		8	
	Ovary	9	SHG shows an increase in collagen fibril/fiber organization
		10	
	Skin	21	SHG can delineate tumor boundaries in different types of skin cancer
		22	
		23	
		24	
Fibrosis	Liver	14	SHG results agree with standard pathology
	Kidney	13	SHG results agree with standard pathology
Connective tissues and disorders	Osteogenesis imperfecta	11	SHG delineates normal and diseased states in several tissue types
	Sjogren's syndrome	12	SHG shows disorganized collagen in this disease
	Cornea	18	SHG can delineate the stroma from other corneal components
		20	
	Skin damage	17	SHG uniquely shows changes in collagen assembly upon thermal damage
Atherosclerosis		15	SHG shows that collagen plaques intermingle with elastin
		16	
Model tissues		19	Self-assembled fibrillar gels can be imaged by SHG
		25	
Theory		26	Theoretical treatments have been developed to understand the SHG emission properties in tissues
		27	
		28	

Research Article

EASL EUROPEAN ASSOCIATION FOR THE STUDY OF THE LIVER | JOURNAL OF HEPATOLOGY

Fibrillar collagen scoring by second harmonic microscopy: A new tool in the assessment of liver fibrosis

Luc Gailhouste[1,7], Yann Le Grand[2,6,7,†], Christophe Odin[2,7], Dominique Guyader[3,7], Bruno Turlin[4,7], Frédéric Ezan[1,7], Yoann Désille[3,7], Thomas Guilbert[2,7], Anne Bessard[1,7], Christophe Frémin[1,7], Nathalie Theret[5,7], Georges Baffet[1,7,*]

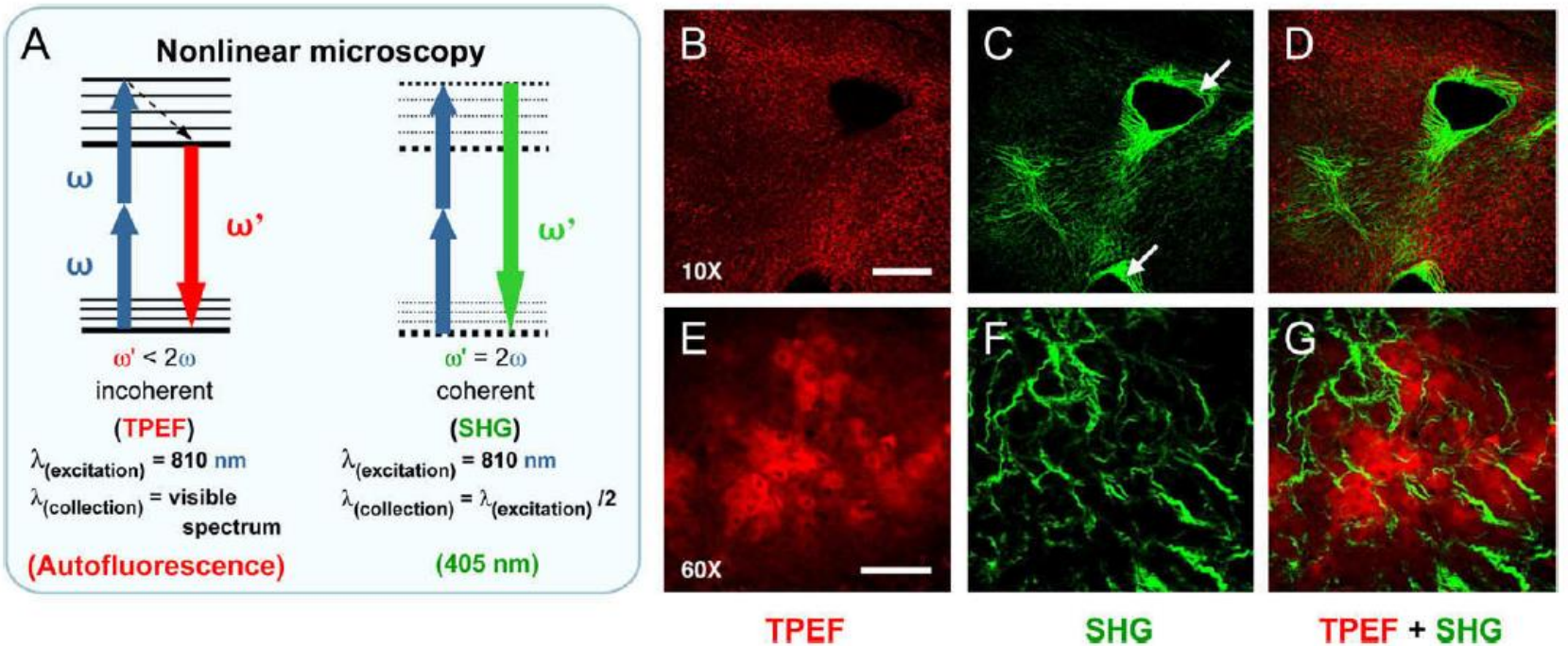

Fig. 1. Nonlinear microscopy in human fibrotic liver. (A) SHG and TPEF imaging principle (energy diagrams) with specific wavelengths of excitation and collection used for acquisitions. (B and E) Typical TPEF recorded with 10× and 60× at mid-depth (50 µm) displayed in red pseudocolor. (C and F) SHG signals collected using a band pass filter at the second harmonic wavelength (405 nm) with 10× and 60×. SHG is shown in green pseudocolor. (D and G) Simultaneous TPEF and SHG imaging. Circular polarization has been used for all acquisitions and laser intensity set at 50 mW (10×) and 25 mW (60×). Scale bars are, respectively, 250 and 60 µm with 10× and 60× magnification.

EASL EUROPEAN ASSOCIATION FOR THE STUDY OF THE LIVER | JOURNAL OF HEPATOLOGY

Fibrillar collagen scoring by second harmonic mici tool in the assessment of liver fibros

Luc Gailhouste[1,7], Yann Le Grand[2,6,7,†], Christophe Odin[2,7], Dominique Guy, Frédéric Ezan[1,7], Yoann Désille[3,7], Thomas Guilbert[2,7], Anne Bessard[1,7], C Nathalie Theret[5,7], Georges Baffet[1,7,*]

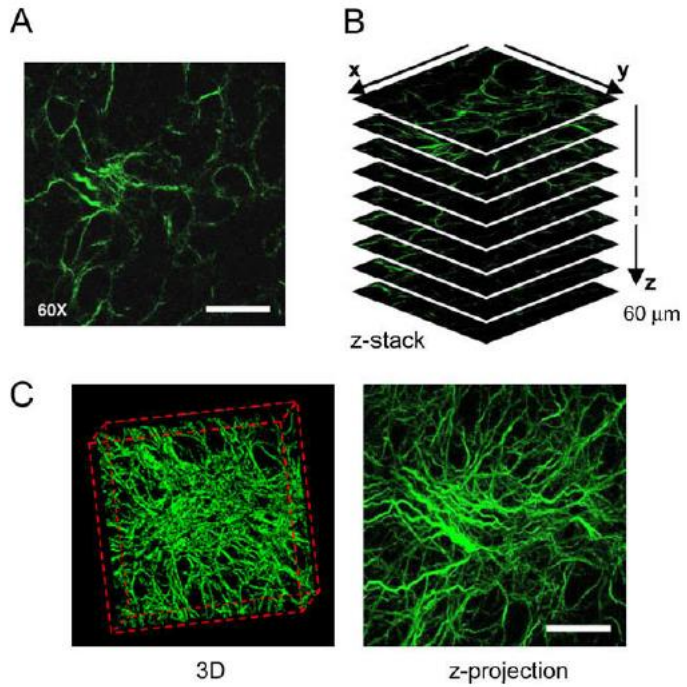

Fig. 2. 3-D imaging by SHG in human fibrotic liver. (A) SHG image recorded at mid-depth of a fibrotic biopsy section. (B) SHG *z*-stack generated with 1 µm step size (0–60 µm deep). (C) ECM network reconstruction in the three dimensions (*xyz*) and *z*-projection of SHG signals collected in the entire volume imaged ($235 \times 235 \times 60\ \mu m^3$). Circular polarization has been used for acquisitions with 25 mW laser input, 810 nm wavelength excitation and 60× objective. Scale bar is 60 µm. See Video S1 for *z*-stack acquisition.

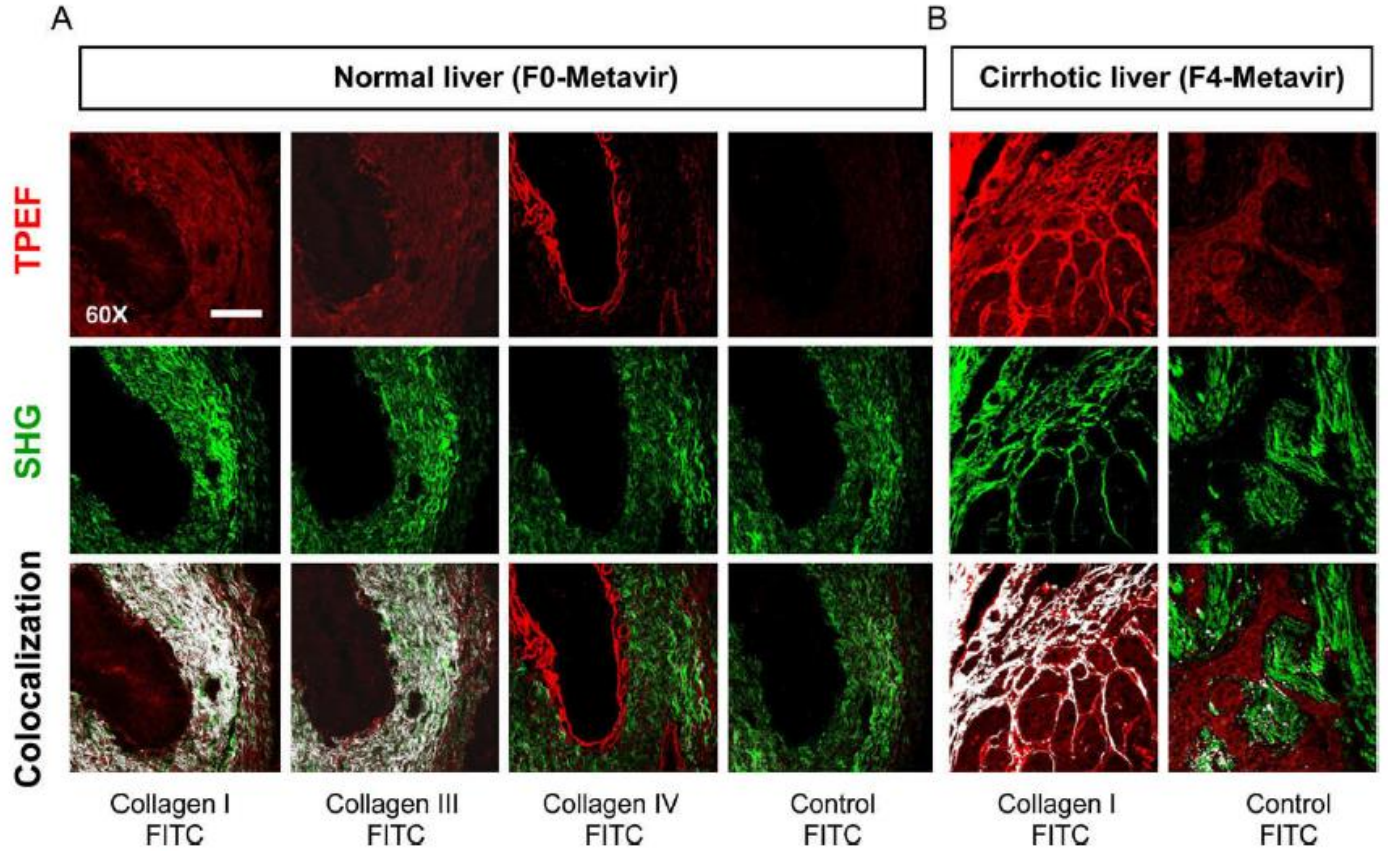

Fig. 3. SHG specificity for fibrillar collagen in liver. The specificity of SHG signals for fibrotic deposits (fibrillar collagen type I and III) in liver has been analyzed by immunohistochemistry assays. (A) Portal area immunolabeling imaged by TPEF and SHG in serial sections of a normal liver (F0-Metavir). (B) Immunoassays performed in highly fibrotic parenchyma of a cirrhotic liver (F4-Metavir). Unlabelled sections have been used as control and colocalization (merging) between SHG and immunostaining (TPEF channel) generated in white pseudocolor. Laser excitation: 25 mW with 810 nm wavelength; 60× objective; Scale bar: 50 µm. See Fig. S1 for fibrillar collagen type III and non-fibrillar collagen type IV immunoassays in cirrhotic samples.

NANO LETTERS

LETTER

pubs.acs.org/NanoLett

3D Nanometer Images of Biological Fibers by Directed Motion of Gold Nanoparticles

Laura C. Estrada* and Enrico Gratton

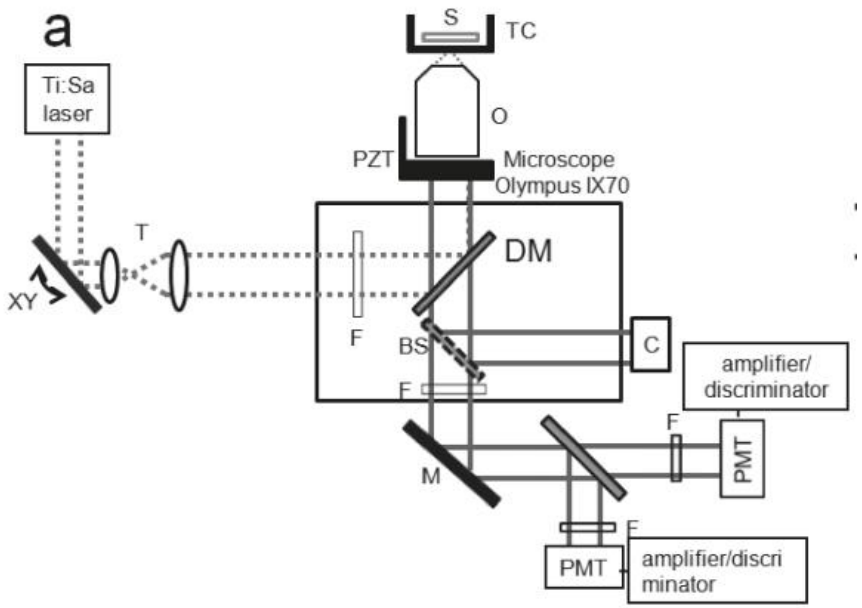

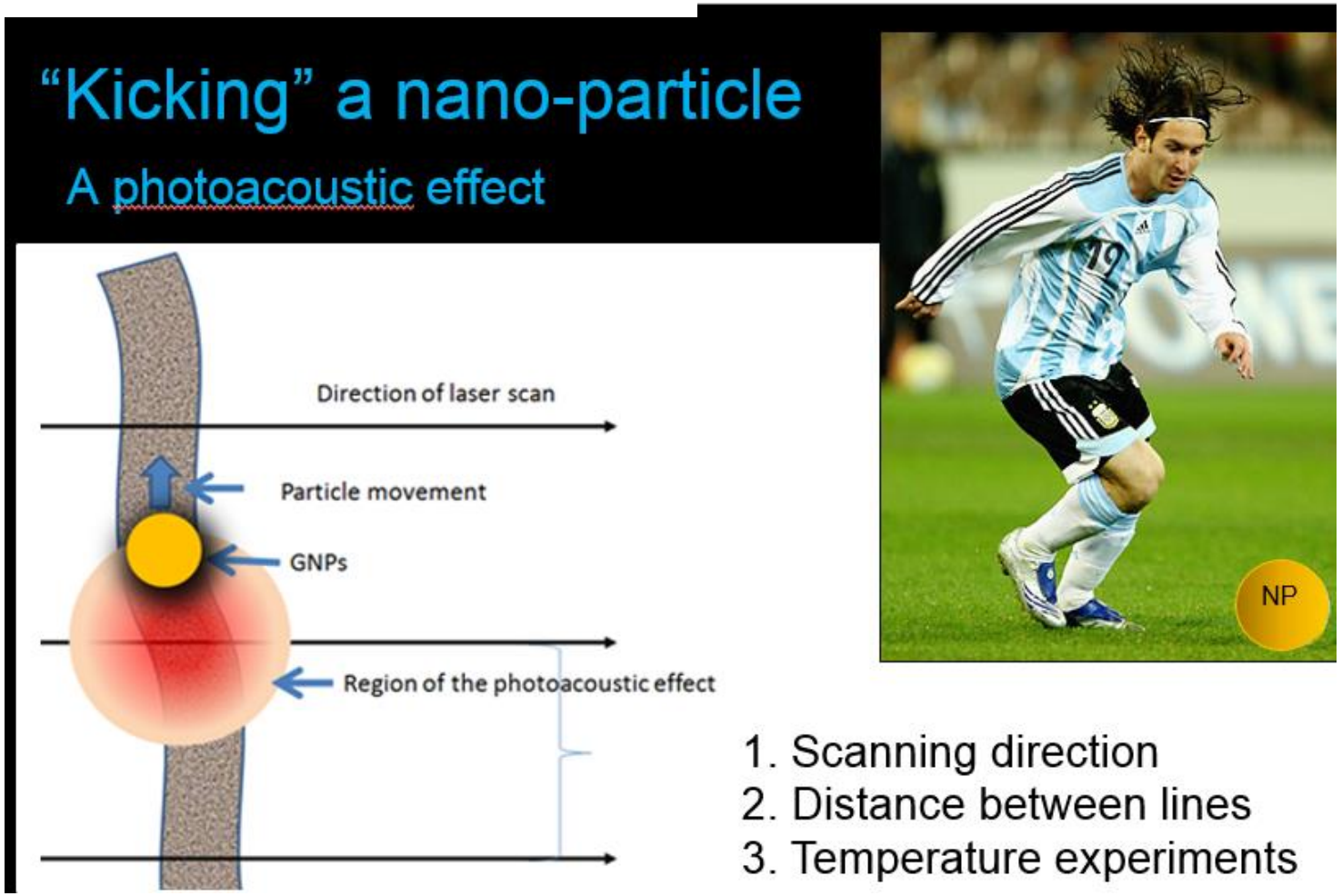

NANO LETTERS

LETTER

pubs.acs.org/NanoLett

3D Nanometer Images of Biological Fibers by Directed Motion of Gold Nanoparticles

Laura C. Estrada* and Enrico Gratton